Tidal range energy resource assessment of the Gulf of California, Mexico

Tidal range energy resource assessment of the Gulf of California, México.

Carlos Joel Mejia-Olivares[1], Ivan D. Haigh[1], Athanasios Angeloudis[2,3], Matt J. Lewis[4] and Simon P. Neill[4]

[1] Ocean and Earth Science, National Oceanography Centre, University of Southampton, European Way, Southampton, SO14 3ZH, U.K.

[2] School of Engineering, Institute for Infrastructure & Environment, University of Edinburgh, Edinburgh, EH9 3FG, UK.

[3] Department of Earth Science & Engineering, Imperial College London, SW7 2AZ, UK

[4]School of Ocean Sciences, Bangor University, LL59 5AB, UK.

Corresponding author

E-mail address: carlos.mejia-olivares@noc.soton.ac.uk (Carlos Joel Mejia-Olivares).
Ocean and Earth Science, National Oceanography Centre, University of Southampton, European Way, Southampton, SO14 3ZH, U.K.

Submit to Renewable Energy

March 2019

Abstract

There has been a growing interest in assessing tidal range energy resources in Latin America as a result of increased demand for electricity. The northern part of the Gulf of California (GC) in Mexico has a relatively large mean tidal range (4m to 5m), and so could be a potential site for tidal range energy exploitation. A detailed quantification of the theoretical tidal range energy resource was performed using tidal level predictions from a depth-averaged barotropic hydrodynamic model and a 0-D modelling approach was used to determine the power that can be technically exploited at four key sites. The results show that the annual energy yield ranges from 20 to 50 kWh/m^2 while the maximum values are between 45 and 50 kWh/m^2 in the vicinity of the Gulf of Santa Clara. This site has the best performing delivering technically annual energy output of 125 GWh (ebb-only), 159 GWh (two-way) and 174 GWh (two-way with pumping) within an impound area of 10 km^2 which are 50%, 40% and 33% of the absolute value power relative to a much-studied reference site (Swansea Bay in the UK). Therefore, a tidal-range power station with a two-way and pumping scheme appears viable for the region.

Key words: Tidal range energy; resource assessment, annual energy yield, technical power; Gulf of California; México.

Highlights

- Gulf of California (México) theoretical and technical energy assessment.
- Predicted peak tidal range between 5 and 8 m at sites in the Gulf of California.
- Theoretical annual energy yield estimates in the northern region were ~ 40 to 50 kWh/m^2.
- Gulf of Santa Clara has the best technical power output performance in the Gulf of California.

1. Introduction

In the last two decades the demand for, and production of electricity has increased significantly [1], driven by urbanization, technological advancement, and high growth in the human population. Since 1975, the global population has grown by almost 2.5 billion and the demand of electricity has more than doubled as a result [2]. Around the world, electricity generation is still heavily dependent on fossil fuels. However, fossil fuels are a finite resource, and there are increasing pressures on thermal power generation relating to climate change. Climate change has resulted in an increase in global temperatures, with many associated negative social, economic and environmental consequences [3]. These two important issues are driving the move towards low carbon renewable energy sources. There is a growing emphasis on identifying alternative and efficient methods to generate the electricity that is essential for the continued economic development and well-being of the world's population. Moreover, clean energies would significantly contribute to reducing greenhouse gases emissions in line with the Paris Climate Change Agreement [4].

Over the last two decades there has been increased interest in tidal energy exploitation [1]. Tidal energy offers many benefits compared to other sources of renewable energy, because of the regular and predictable nature of ocean tides [5]. There are two main forms of tidal energy. First, tidal-stream energy, which exploits the kinetic energy of tidal currents, through the deployment of devices that are able to convert the horizontal velocity of the ocean's currents into a rotational torque [5]. Secondly, tidal range energy, which exploits the potential energy from the water-level differences between two bodies of water, over the rise and fall of the tide, through the impounded area of sea water into a reservoir as a result of the construction of tidal barrages or lagoons [6] and [7]. Consequently the dam flow is directed into a hydrodynamic turbine producing mechanical motion due to the flow that cross along the area of the turbine.

In this paper we focus on tidal range energy, which has a long history. Tidal mills have utilised tidal energy to operate for at least the last 800 to 900 years [8]. However, the first large-scale commercial tidal range energy project was the La Rance Tidal barrage in France commissioned in 1967. Subsequent schemes in operation include Kislaya, Gubska in Russia [9], the Lake Shiwa in South Korea [9], [10] and [11], Jiangxia in China [12] and Nova Scotia in Canada [9]. These schemes all involved the construction of large barrages in tidal inlets or bays [13]. There are a host of additional areas that have been identified as being

suitable for tidal range energy extraction and these are summarised in [14]. They found that the bulk of the global tidal range energy resources are distributed among Canada (23%), Australia (30%), UK (13%), France (13%), US (11%), Brazil (5%), South Korea (2%), Argentina (1%), Russia (<1%), India (<1%) and China (<1%). There is also increasing scope in utilising small bays and lagoons for tidal energy extraction, such as the proposal for a Swansea Bay tidal lagoon project in the UK [9], these schemes aim to balance electricity production and the potential hydro-environmental implications of larger tidal barrage schemes that have been considered to-date. In the article by [14] the authors estimated that the global annual theoretical potential tidal range energy resource is ~25,880 TWh.

The demand for electricity in Latin America has increased considerably in recent decades due to substantial economic development and population growth [15]. This paper focuses on Mexico, which is the second largest country in Latin America (after Brazil). Mexico's crude oil reserves ranks within the top 10 in the world [15], and its electric power consumption per capita is approximately 2,090 kWh while, for comparison, the USA and the UK the electricity power consumption per capita is 12,984 kWh and 5,129 kWh respectively [16]. Further, in 2014 the mean electricity power consumption per capita in the world was reported as 3,128 kWh [16]. In 2012 and 2013, Mexico consumed approximately 260 TWh and 220 TWh of electricity, respectively. 80% of the electricity produced in Mexico is sourced from thermal power plants and, as a result, the country is highly dependent on the combustion of fossil fuels [17]. In 2013, total carbon dioxide (CO_2) emissions from electricity production in Mexico was approximately 133 million metric tons [18]. However, Mexico has set an ambitious goal of generating 35% of its total electricity from renewable sources by 2027 and thus lowering its carbon emissions [18]. To date, 19% of Mexico's electricity is generated by renewable energy resources such as solar, wind turbines, biomass, geothermal and hydropower energy [15]. Currently, no electricity is generated through the tides in Mexico.

In a companion study by [19], we undertook a detail tidal-stream energy resource assessment for the Gulf of California (hereafter GC) in Mexico (Fig. 1a). Here, we focus on assessing the theoretical tidal range energy resource in the northern part of GC which has a relatively large spring tidal range (7-8m). To-date, two studies [20] and [21] have identified sites in the GC with significant potential for tidal range energy conversion.

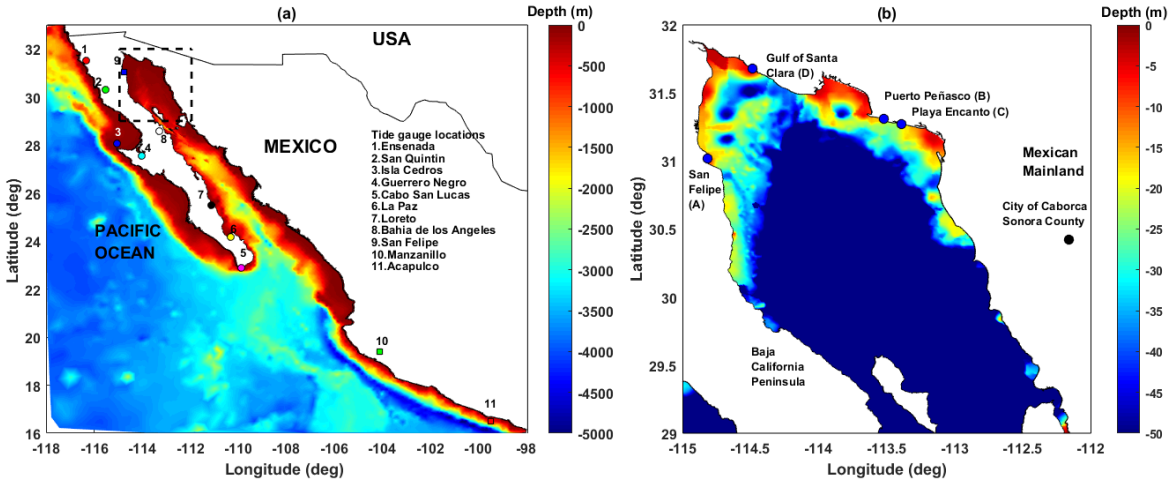

Fig. 1: Location of the study area with water depths for the: (a) Gulf of California, with the locations of the tide gauge sites; and (b) the Northern Gulf of California.

In the study by [20] assessed the feasibility and potential tidal range energy resources for a tidal barrage situated at San Felipe port in the northern-most reaches of the GC. Using the predictions from a numerical hydrodynamic model (not described in the report cited), they extracted predicted water level time series at San Felipe port. Furthermore, they estimated the theoretical annual electricity production of 17 325 GWh suggesting a basin area of 2,590 km^2. Thus, this basin area would have to be impounded by constructing a barrage of more than 72 km in length from San Felipe port at the Baja California Peninsula to Puerto Peñasco (Fig. 1b).

Another study was undertaken by [21], they identified several potential sites suitable for tidal range energy extraction, including in the bays of: (i) Santa Maria near San Felipe port, (ii) San Luis Gonzaga southern San Felipe port, (iii) Los Angeles bay, (iv) El Pescador southern Los Angeles Bay, (v) El Soldado at the Bay of las animas, and (vi) San Rafael opposite San Lorenzo Island. Sites (i) and (ii) are situated in the northern reaches of the GC, and (iii) to (vi) are in the Midriff area. In the study by [21] estimated the theoretical tidal range energy resources using predictions from a three-dimensional numerical model of the GC, configured using the Hamburg Shelf Ocean model (HAMSOM) developed by Backhaus [22] [23] and adapted by [24] and [25]. In calculating the resource, they used a theoretical approach and assumed losses due to turbine efficiency. Their results suggested that a 6.87 km^2 scheme in the Bay of Santa Maria could generate 2.56 MW of electricity with a total energy extraction of 9.48 GWh/year.

Results from these two studies indicate that the northern part of the GC has sites with potential for tidal range energy extraction. However, considering the differences in estimated power between these two studies, the need for renewable energy power stations in the region, and recent developments in tidal range power modelling (e.g. [26][27]) the tidal range resource of the region ought to be revisited to understand the potential contribution it could make to Mexico's renewable energy targets.

The overall aim of this paper is to undertake a detailed quantification of the tidal range energy resource in the northern reaches of the GC. To address this there are three objectives, as follows:

1. To map how the tidal range varies in the northern part of the GC;
2. To estimate the theoretical annual potential energy density in this region and how this resource varies subject to different bathymetry datasets while accounting for multiple tidal constituents; and
3. To determine the available energy that can be technically extractable whilst considering different operational strategies and certain tidal power plant technical specifications.

The structure of this paper is as follows. Section 2 provides a brief overview of the model configuration (previously set up by [19]) and validation. Section 3 outlines the methodology used to assess the available power density and theoretical annual energy yield in the northern GC. The results for each of the three objectives are then described in Section 4. Key findings are discussed in Section 5 and conclusions provided in Section 6.

2. Gulf of California Model Configuration and Validation

In this study we employ the depth-averaged barotropic model for the GC configured by [19]. Here, we briefly describe the model setup (Section 2.1) and comparisons of model output with measured water level data (Section 2.2), but also direct the reader to the more detailed description of the model configuration and validation provided in [19].

2.1 Model configuration

The model was configured using the TELEMAC modelling suite [28]. TELEMAC is a popular model choice for tidal energy resource assessment characterization, mainly, due to

the variable mesh resolution (e.g., [29], [30] and [31]). The generated model mesh has a resolution of 0.507° (~60 km) along the open boundary in the Pacific (Fig. 2a) and increases to 1/120° (~1 km) along the coastline in the northern reaches of the GC (Fig. 2b). The bathymetric data interpolated onto the mesh was downloaded from the General Bathymetry Chart of the Oceans [32] at a 30 arc-second resolution (~900 m). Higher resolution (~450 m) bathymetry data in the northern GC (obtained from The Center for Scientific Research and Higher Education at Ensenada; CICESE; (http://www.cicese.edu.mx), was merged within the GEBCO gridded data (both relative to mean sea level). As a sensitivity test we ran a simulation with the bathymetry defined using ETOPO bathymetry data [33], and this is discussed later in the paper. The open ocean boundary was driven with tidal levels derived from the Oregon State University Tidal Inversion Software (OTIS) TPXO 7.2 database [34] [35] using eight principal (M_2, S_2, N_2, K_1, O_1, P_1, Q_1), three non-linear (M_4, MS_4, MN_4) and two long period (Mf, Mm) tidal constituents. A constant spatial uniform Manning's friction number of 0.030 $s/m^{1/3}$ was used.

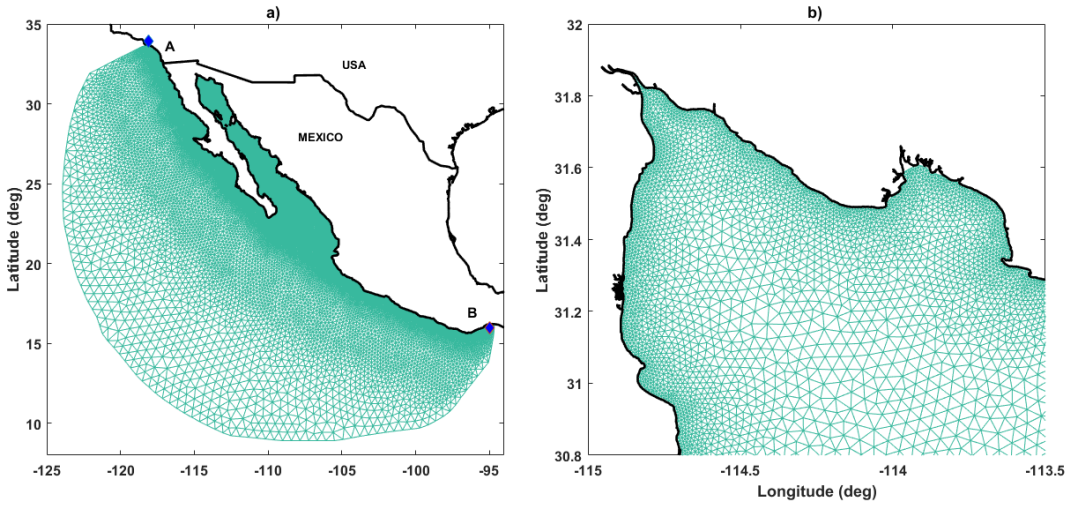

Fig. 1: (a) Domain area model of the Gulf of California (b) Northern GC

2.2 Model Validation

The model has been extensively validated against tide gauge and ADCP measurements to ensure hydrodynamic conditions are accurately reproduced in the GC (please see reference [19] for detailed description). Predicted tidal levels were compared against measured water levels at 11 tide gauge sites in the region, the locations of which are shown on Fig. 1a. The tide gauge datasets were obtained from CICESE. We undertook a harmonic analysis of the

tide gauge records using the T-TIDE software [36] to extract the astronomical tidal component. Time-series comparison of the measured and predicted tidal levels are shown in Fig. 3 for December 2013, revealing good agreement at all sites. The largest differences are at La Paz (site 6 in Fig. 1a) which is located in an enclosed bay with a complex bathymetry that is not accurately represented at our present model resolution (3 km in this region).

We calculated the differences between the amplitude and phases of the main tidal constituents and used three error metrics to statistically assess model performance (Table 1) (again please see reference [19] for further details). In summary, mean amplitude differences across the 11 validation sites were less than 7 cm for the main constituents, with the exception of K_1 which had an average difference of 20 cm. The mean phase differences were 10° or less for M_2 and O_1, and were less than 21° different for the remaining constituents. For each of the time-series (shown in Fig. 3), the absolute difference between each hourly measured and predicted value was computed. The mean, equivalent to the root mean square error (RMSE) and standard deviation of the absolute differences were calculated and correlation coefficients between the measured and predicted time-series were also derived. The largest RMSE was predicted at Guerrero Negro (0.25 m) while the smallest were at Ensenada (0.03 m), Cabo san Lucas (0.06 m) and Loreto and Manzanillo (0.07 m) (Table 1). The mean standard deviation across the validation sites was 0.078 m. The mean correlation coefficient was 0.94. In general, these results demonstrate that the model performs well in reproducing tidal levels in the GC.

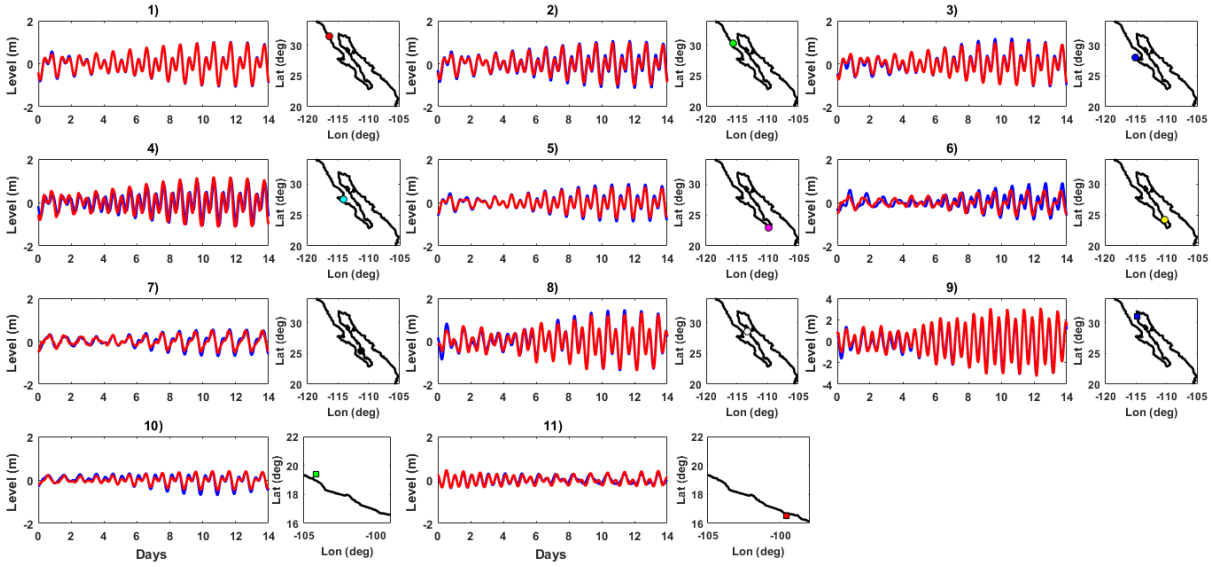

Fig. 3: Comparison of the measured (blue) and predicted (red) tidal time-series at: (1) Ensenada; (2) San Quintin); (3) Isla Cedros; (4) Guerrero Negro; (5) Cabo San Lucas (6) La

Paz; (7) Loreto; (8) Bahia de los Angeles; (9) San Felipe; (10) Manzanillo; (11) Acapulco. Reference numbers based on Fig. 1 sites list.

Table 1: Statistical validation error measures for the 11 tide gauge stations including all model tidal constituents of the simulation. See [19] for the time period used for the validation.

Site number	**Site Name**	**RMSE (m)**	**% Error**	**STD (m)**	**Correlation Coefficient**
1	Ensenada	0.03	1.2	0.02	0.99
2	San Quintin	0.11	4.5	0.07	0.97
3	Isla Cedros	0.10	4.4	0.09	0.96
4	Guerrero Negro	0.26	9.6	0.15	0.84
5	Cabo San Lucas	0.06	3.0	0.04	0.99
6	La Paz	0.19	10.9	0.12	0.75
7	Loreto	0.08	5.9	0.05	0.95
8	Bahia de los Angeles	0.09	3.0	0.07	0.98
9	San Felipe	0.25	3.8	0.17	0.99
10	Manzanillo	0.07	6.1	0.05	0.94
11	Acapulco	0.07	7.7	0.05	0.91
All	**Mean**	**0.11**	**5.0**	**0.07**	**0.86**

3. Methodology for resource characterization

In this section, we describe how we have used the validated model to assess tidal levels and estimate the energy resources of the region, including undertaking sensitivity tests using different bathymetry sources in the model and varying numbers of tidal constituents.

3.1 Tidal level analysis

Using the validated model, tidal levels across the GC were assessed, with a focus on the northern region, to determine the location of the highest tidal levels and how they vary over

time. The model was run for the period 27 November 2015 to 31 December 2015 and results were stored at every grid point every 10 minutes. The first three days were considered as the warm up period and were discarded from the analysis. At each element node a harmonic analysis was undertook on the monthly predicted tidal level time-series using the T-TIDE software [36]. We then used the tidal harmonics to predict tidal levels for a full year, which saved the computation expense of running the high-resolution model for a year. Then the annual maximum and mean tidal range from the annual time-series at the element nodes were calculated. We compared this to the maximum and mean tidal range, computed using just the combined M_2 and S_2 tidal constituents.

3.2 Methodology to assess the theoretical power density and annual energy yield

Next, we quantified the theoretical energy density (per m^2) in the GC with a focus on the northern region because the highest tidal levels were observed here. The energy was estimated following the approach of [6] in which the theoretical potential energy is given by:

$$E = \frac{1}{2}\ \rho g A\ h^2 \quad \text{(units in J)} \qquad \text{(EQ1)}$$

Where A is the area of the impounded basin, ρ is the density of sea water (1025 kg/m^3), g is the acceleration due to gravity (9.81 m/s^2), and h (in m) is the head, normally defined as the water level differences between HW (high water) and LW (low water) peaks of a tidal elevation time series. The annual energy yield resource per m^2 (E_{annual}) was then calculated as follows:

$$E_{annual} = \sum_{i=1}^{n} \left(\frac{1}{2}\rho g A {h_i}^2\right) \quad \text{(units J)} \qquad \text{(EQ2)}$$

Where n is the accumulated water transitions from HW to LW, or LW to HW. The potential energy estimated by Eq. (1) was divided by the impounded area to produce a metric that represents the spatially varying potential energy (i.e., the energy density, as $E = {}^1/_2\,\rho g h^2$ in J/m^2).

In order to calculate the annual energy yield (per m^2) using Eq. (2), the head h was first extracted from each transition from high to low water and vice versa, from the elevation-time-series. In turn it was used to calculate the energy density for each consecutive flood and ebb tide and then accumulated for 1,411 cycles that are expected in a year.

We then undertook a series of sensitivity tests in which we estimated and compared the theoretical energy density for time-series derived using all available tidal constituents (analysing monthly tidal predictions with T-TIDE gave 29 tidal constituents) and then just for the main semi-diurnal constituents, M_2 and S_2. We also compared energy estimates from model runs that used: (1) just the GEBCO bathymetry; (2) just the ETOPO bathymetry; and (3) the GEBCO data merged with the higher resolution data from CICESE in the northern part of the GC.

3.3 Methodology to assess the technically extractable energy

Finally, we determined the energy that can be technically converted, whilst considering different operational strategies and certain tidal power plant technical specifications. The performance of a tidal-range power plant can be evaluated once a tidal signal is available that can be sufficiently representative of the outer water level evolution that the hydraulic structures will experience once the plant is constructed [14]. For an early-stage assessment, this can be done in a manner that omits the influence of the structure on the localised hydrodynamics and assumes a constant impounded surface area with negligible water elevation variations in its interior [6]. This approach is known as 0-D modelling and has been applied on several occasions to assess the performance of tidal-range schemes [37], [38], [39]. Our tidal power plant operation simulations employ a finite difference 0-D model based on the principles of continuity as implemented in [40], building on earlier operational modelling studies from [41] and [42]. Operation sequence algorithms dictate the flow through hydraulic structures and by extension (in the case of turbines) the power produced or consumed while pumping. There are multiple ways of operating a tidal power plant, as summarised in the schematics of Fig. 4 which were produced using the parameters summarised in Table 2. For a more detailed description of the ebb-generation and two-way generation, the interested reader is directed in [43] and for two-way generation with pumping see [38].

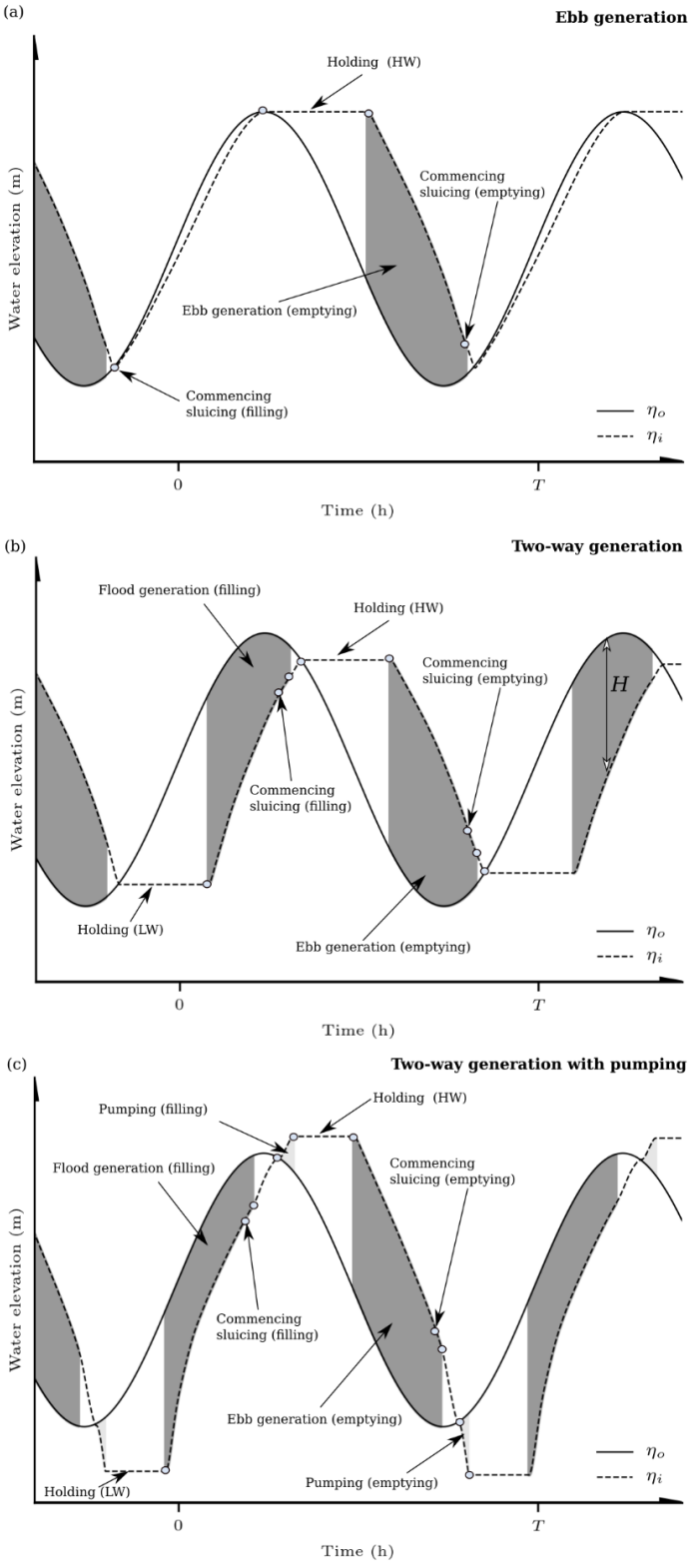

Fig. 4: Typical operation strategies for a tidal power plant as simulated by our 0-D model: (a) one-way ebb generation, (b) two-way generation, (c) two-way generation with pumping. η_o is the outer water elevation in the seaward side of the hydraulic structures while η_i is the inner water elevation within the tidal power plant.

Table 2: Operational parameters used for the 0-D operational model for typical operational strategies employed in tidal range power plants. EBB = One-way ebb generation, TW = Two-way generation, TWP = Two-way generation with pumping.

Operation specifications	**Notation**	**EBB**	**TW**	**TWP**	**Units(hours)**
Holding duration (ebb/flood)	$t_{h,e}$, $t_{h,f}$	3.50 / 0.00	3.00 / 3.00	2.00 / 2.00	h
Pumping duration (ebb/flood)	$t_{p,e}$, $t_{p,f}$	0.00 / 0.00	0.00 / 0.00	0.50 /0.50	h
Max Generation w/o sluicing (ebb/flood)	$t_{g,e}$, $t_{g,f}$	6.00 / 0.00	3.00 / 3.00	3.00 / 3.00	h

Our approach hypothesises the deployment of a tidal lagoon plant at four sites of interest (Gulf of Santa Clara, San Felipe, Puerto Peñasco and Playa Encanto), the locations of which are shown in Fig. 1b. We pre-selected these four locations as the mean tidal range here was greater than 4 m within water depths less than 20m which are suitable for the construction of a lagoon and they are located close to Mexican electrical grid points, as discussed later in Section 5. A constant upstream surface area of 10 km^2 is assumed as in [42].This entails a scenario that would be expected for offshore tidal lagoon schemes as they would not be influenced by intertidal areas. (e.g. [44]). As a result, the water volume impounded is assumed to linearly vary with the water depth h. The impounded area A = 10 km^2 corresponds to a relatively small-scale tidal range scheme. For example, the 320 MW Swansea Bay tidal lagoon project within the Bristol Channel, UK, has been perceived as a pilot-scale project with a maximum surface area of 11.6 km^2 [9].

The formulations employed for the flow through hydraulic structures at every time step are outlined in [40] involving the orifice equation for sluice gates using a discharge coefficient of C_D = 1.0 (consistent with the sensitivity study of [45]) and a sluice gate cross-sectional area of A_s = 100 m^2. For the turbine parametrisation, representative hill charts are required to incorporate the performance of low-head bulb turbine designs; this technology is typically installed for power generation from tidal range structure proposals. The calculation process followed for the hill chart has been described by [46]. In particular, we assume that generation will be facilitated by turbines with a capacity of 20 MW, a diameter D = 7.35 m in accordance with recent UK tidal range energy studies [27], [47], [9]. In Fig. 5 the calculated

20 MW turbine hill chart is plotted together with an idealized representation from first principles. The idealized representation omits efficiency factors acknowledged by the hill chart and demonstrates how lower flows are predicted to generate an equivalent amount of power depending on the head difference *h* subjected to the turbine. A comparison between the two curves also suggests significant efficiency losses when generating at relatively low head differences; further compromising the generation during neap tides when *h* facilitated would be relatively lower. Moreover, the algorithms account for a minimum head difference that will be required to generate any electricity, where in this case we assume that h_{min} = 1 m.

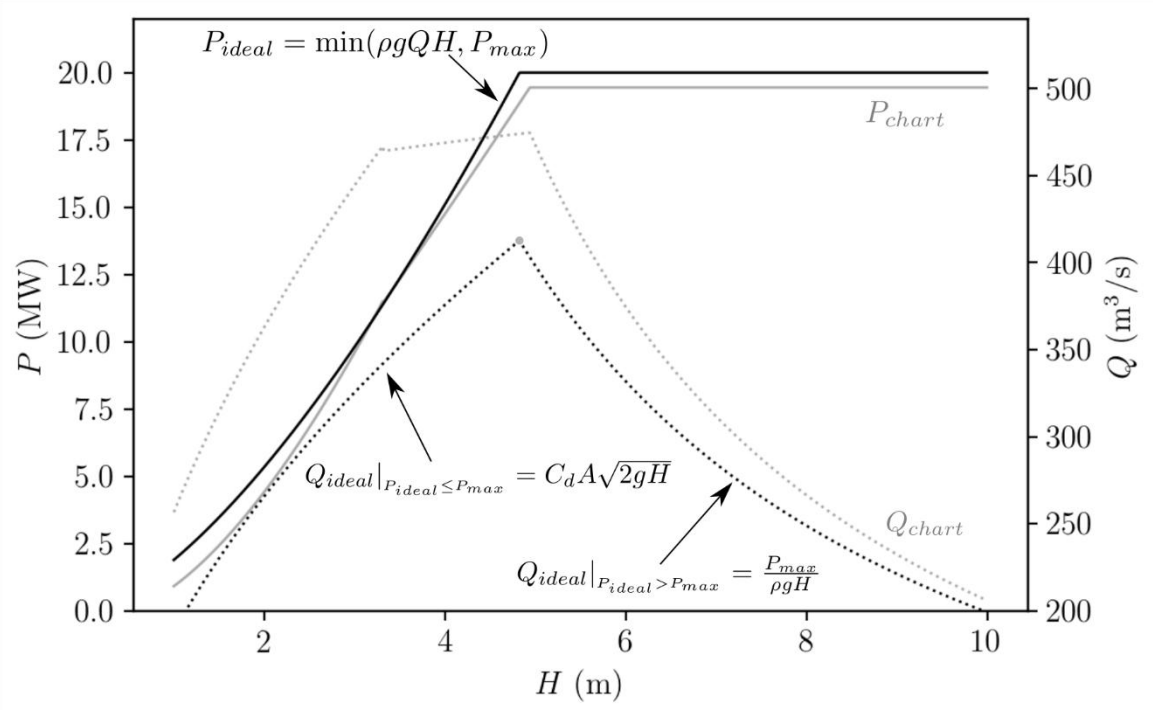

Fig. 5: Idealized and calculated hill chart based on [46]. The hill chart Power (Pchart) and Discharge (Qchart) refers to a 20 MW 7.35 m diameter turbine as per the implementation of [40]. For the idealized hill chart, Cd is the discharge coefficient (=1.0), Pmax = is the turbine capacity (=20 MW) and AT the cross-sectional area of the turbine (assumed to be = π 7.35^2 /4 m^2) and H the head difference.

In the absence of detailed information about specific schemes at the potential sites in Fig. 1(b), certain assumptions must be included in relation to the tidal power plant configuration. Namely, the optimum number of turbines and sluice gates will vary for schemes at different locations according to the available potential energy, amongst additional constraints of a geomorphological, environmental and electrical nature. For our preliminary assessment we formulate the following expression to estimate the capacity *C* (in W):

$$C = \eta \frac{\rho g A \bar{H}^2}{T\ CF} \quad \text{(EQ3)}$$

Where η is the overall generation efficiency, T = 44712 s is the tidal period, CF is the capacity factor and $\bar{H}$ is the mean annual tidal range. It is generally acknowledged that approximately 27 – 55 % of the available energy resource can be harnessed [37], [40]. We thus assume that the maximum potential energy that can be harnessed is subject to an efficiency of η = 0.55. The capacity factor of conventional single-basin tidal range structures can accordingly vary between 0.15 – 0.25 depending on the operation performance. We assume that any proposed scheme in the GC will aim for a value of CF = 0.15. In turn, the number of turbines N_t will be = C/P_{max} and assume for the sluice gate number $N_s = N_t/2$. These parametric relationships have been applied here on an empirical basis and site-specific optimisation that will be essential for more comprehensive practical studies that also acknowledge the site bathymetry, marine spatial planning, economic and environmental constraints.

4. Results

The results of this paper are presented in three parts, each addressing one of the three study objectives (Section 1).

4.1 Tidal range variation

The first objective was to map how the tidal range varies in the northern part of the GC. The annual maximum and annual mean tidal range is shown in Fig. 6a and b, respectively. In the vicinity of the Midriff Islands the maximum tidal range is in the order of 2 m. The tidal range then increases moving north due to effects of tidal resonance that amplify the tidal wave as it propagates towards the northern coast, facilitating a maximum during spring tides of approximately 8 m in the northern most part of the Gulf (Fig. 6a). The mean tidal range is of order 4 to 5m in the northern most part of the Gulf (Fig. 6b and Table 3 and 4). The annual maximum and annual mean tidal range, calculated just using the M_2 and S_2 tidal constituents, are shown in Fig. 6c and d. When we consider just the M_2 and S_2 tidal constituents the annual maximum tidal range reduce significantly from 8 to 5 m in the northern part of the Gulf (Gulf of Santa Clara region) while the annual mean tidal range reduces from 5 to 4 m.

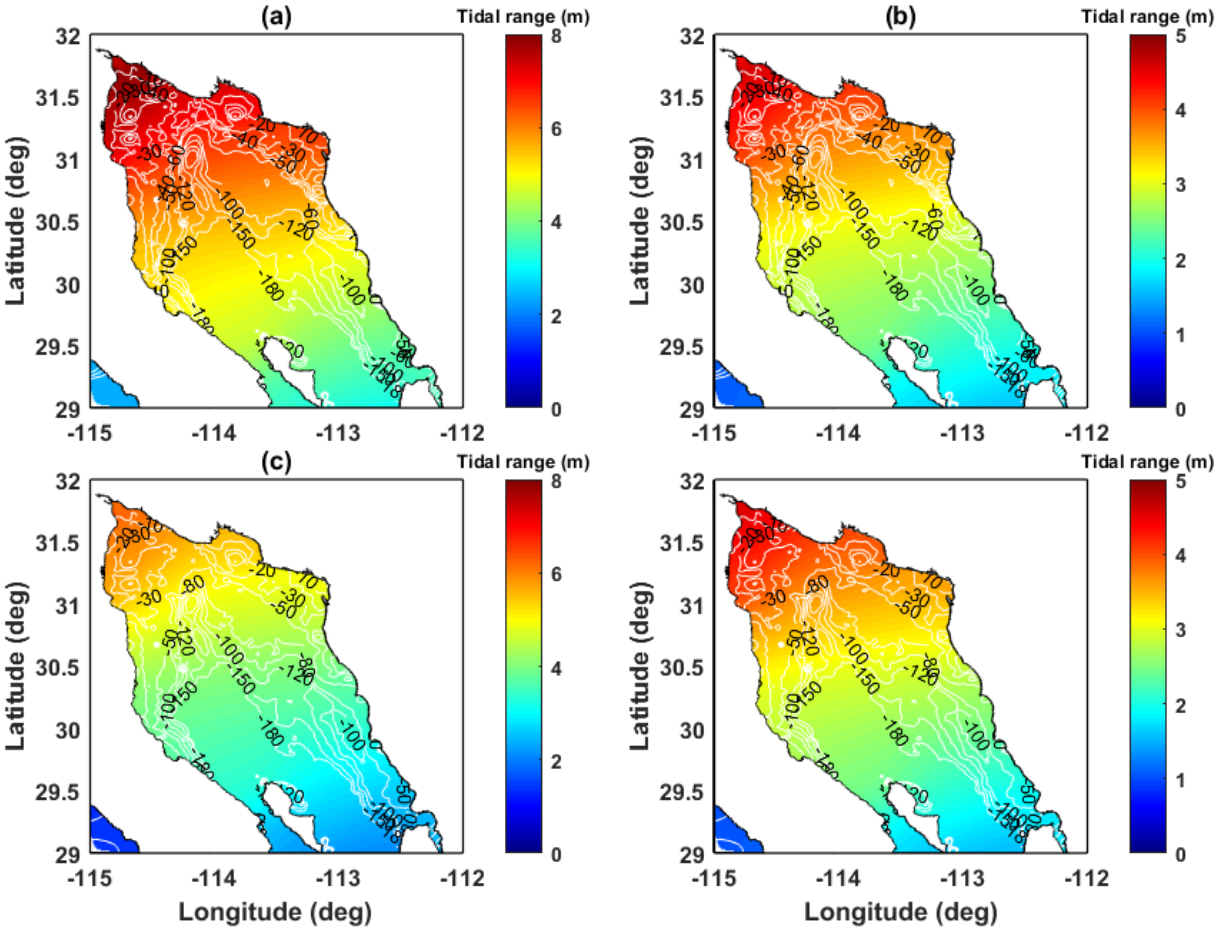

Fig. 6: (a) Maximum tidal range and (b) mean tidal range all model constituents, (c) Maximum tidal range and (d) mean tidal range using predicted tide with M_2 plus S_2 tidal constituents. All plots use the GEBCO data merged with the higher resolution data from CICESE, for the northern Gulf of California, with the bathymetry contours are overlaid as white lines.

Table 3: Summary of sites considered for operational models in the Gulf of California, and a reference site based on the UK where tidal range projects have been considered. The table summarises, the mean tidal range, the annual energy per unit area, and the installed capacity calculated based on Eq3.

#	Site Name	Latitude (^{o})	Longitude (^{o})	$\overline{H}$ (m)	E_{yr}/A (GWh/km^2)	C/A (MW/km^2)
A	San Felipe	31.088	-114.740	4.37	45.2	15.8
B	Puerto Peñasco	31.287	-113.675	4.05	38.6	13.5
C	Playa Encanto	31.264	-113.812	4.08	39.2	13.7
D	Gulf of Santa Clara	31.489	-114.477	4.59	49.8	17.4
Reference	**Swansea Bay**	**51.58**	**-3.90**	**6.61**	**94.7**	**36**

Table 4: Practical annual energy output and operational efficiency for tidal range energy schemes at the selected sites along the coast of the Gulf of California. Table includes results from a reference site in the UK that has been identified as feasible for the deployment of the technology. In all cases the impounded area is = 10 km^2.

#	Site Name	Ebb-only (EBB)		Two-way (TW)		Two-way with pumping (TWP)	
		E_{yr} (Gwh)	η (%)	E_{yr} (GWh)	η (%)	E_{yr} (GWh)	η (%)
A	San Felipe	112	24.8	133	29.7	144	31.9
B	Puerto Peñasco	93	24.1	100	25.9	104	27.1
C	Playa Encanto	94	24.1	103	26.3	108	27.5
D	Gulf of Santa Clara	125	25.1	159	32	174	35
Reference	**Swansea Bay**	**250**	**26.4**	**393**	**41.1**	**520**	**55**

4.2 Energy density and annual theoretical resource

The second objective was to estimate the theoretical potential energy density as well as the theoretical annual energy yield in this region, and how this resource varies subject to different bathymetry datasets while accounting for multiple tidal constituents. The annual maximum and annual mean energy density for the region are shown in Figs. 7a and b, respectively. Energy density varies spatially and reflects, as expected, the spatial distribution of tidal range, shown in Figs. 6a and b. The maximum values are located at the upper Gulf (opposite Gulf of Santa Clara) and are around 0.1 kWh/m$^{2.}$ The water depth at these locations is less than 30 m. The power density is much lower around the Midriff region, ranging from 0.03 and 0.04

kWh/m^2. Here water depths vary between 40 to 180 m. The annual mean energy density in the upper Gulf is between 0.035 and 0.040 kWh/m^2 while in the middle and lower northern GC it is smaller, between 0.025 and 0.018 kWh/m^2, respectively.

We also, again for comparison purposes, estimate the annual maximum and mean power density using predicted tidal level time-series considering just the M_2 plus S_2 tidal constituents and results are shown in Figs. 7c and d. Comparing Fig. 7a with Fig. 7c, the maximum power density is almost halved when just considering tidal levels predicted just using the M_2 plus S_2 tidal constituents, from 0.09 to 0.05 kWh/m^2. The mean energy density reduces from 0.035 to 0.030 kWh/m^2 (Fig. 7b and d).

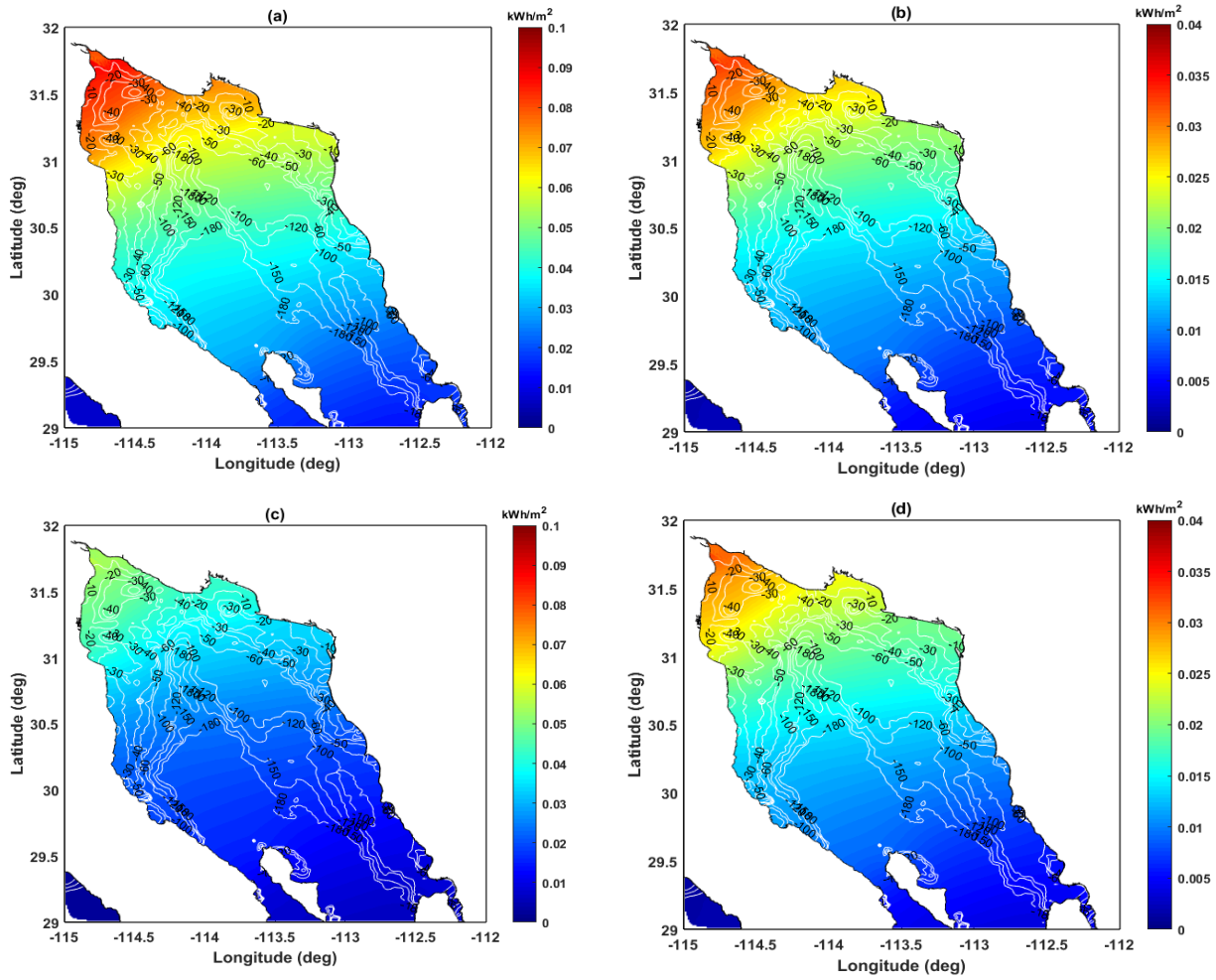

Fig. 7: Max energy density (a) all model constituents (c) Using only M_2 plus S_2 tidal constituents. Mean energy density (b) all model constituents (d) Using only M_2 plus S_2 tidal constituents. All plots use the GEBCO data merged with the higher resolution data from CICESE, for the northern Gulf of California, with the bathymetry contours are overlaid as white lines.

Time series of tidal levels and potential energy density (calculated as instantaneous contributions from each transition of HW to LW and *vice versa)* are shown in Fig. 8a to 8d for four sites in the GC (the locations of which are shown in Fig. 1). We consider that these areas have potential for constructing a tidal range power plant, as the mean tidal range exceeds 5 m and the topography and water depth are appropriate for the construction of a lagoon. The mean annual power density in those locations is in the range of 0.015 to 0.038 kW/m^2.

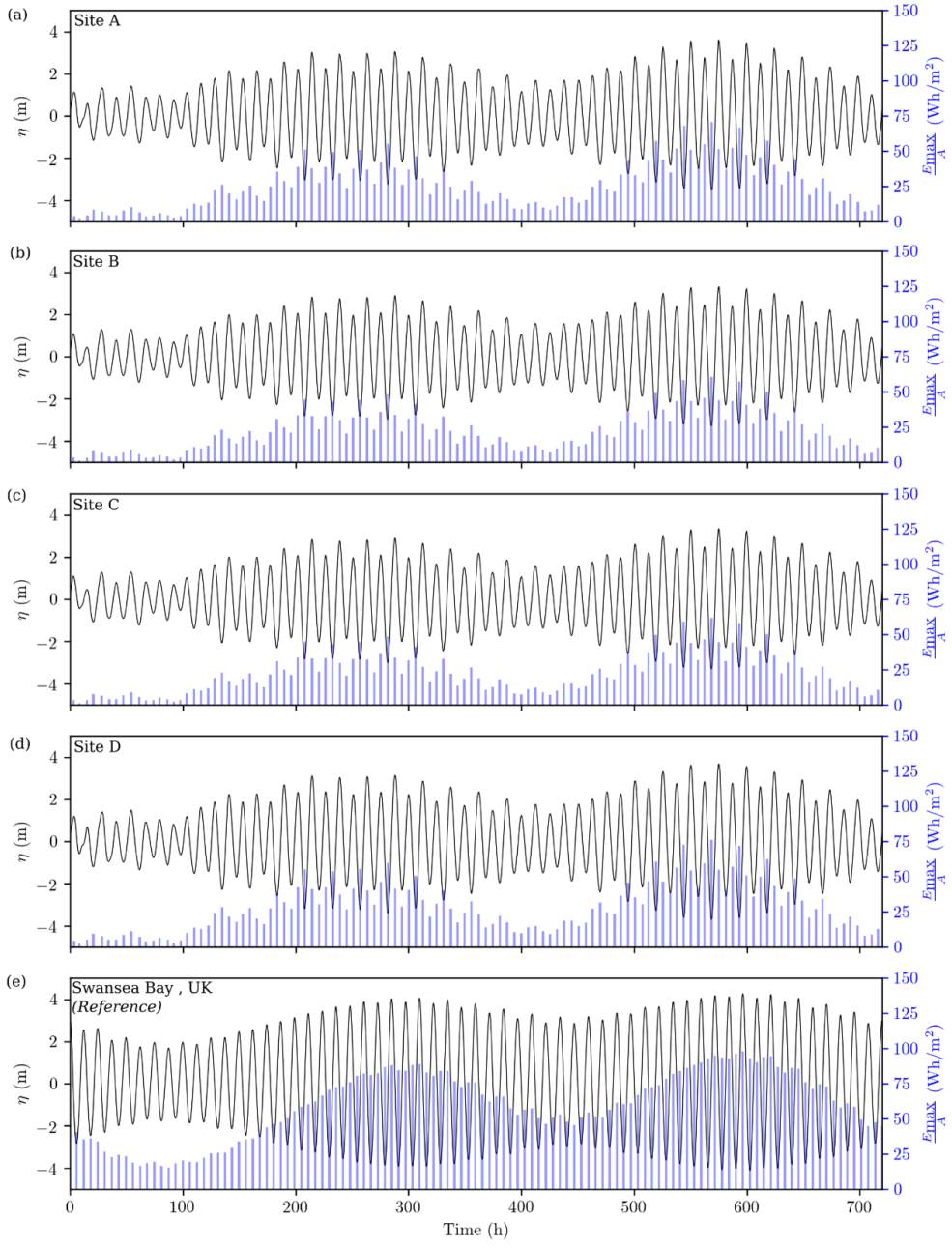

Fig. 8: Monthly energy density and tidal levels at (a) San Felipe, (b) Puerto Peñasco, (c) Playa Encanto, (d) Gulf of Santa Clara and (e) Swansea Bay, UK. The latter is used as a reference for a tidal energy project that has been considered in the Bristol Channel considered as feasible.

We also estimated the theoretical annual energy yield and the results are shown in Fig. 9a. The potential annual energy yield ranges from 20 to 50 kWh/m^2. The maximum values are in the northern region of the GC and are around 45 and 50 kWh/m^2 in the vicinity of the Gulf of Santa Clara. At Puerto Peñasco, San Felipe and Playa Encanto the annual yield energy is lower, ranging from 30 and 35 kWh/m^2. In the southern reaches of the northern GC the annual yield energy is lower, between 20 to 25 kWh/m^2. In a similar way, we compared the annual yield energy based on annual tidal predictions estimated using only the M_2 and S_2 tidal constituents (Fig. 9b). On average, the resource is 10 to 13 kWh/m^2 higher when considering all tidal constituents analysed, compared to the consideration of M_2 and S_2 alone.

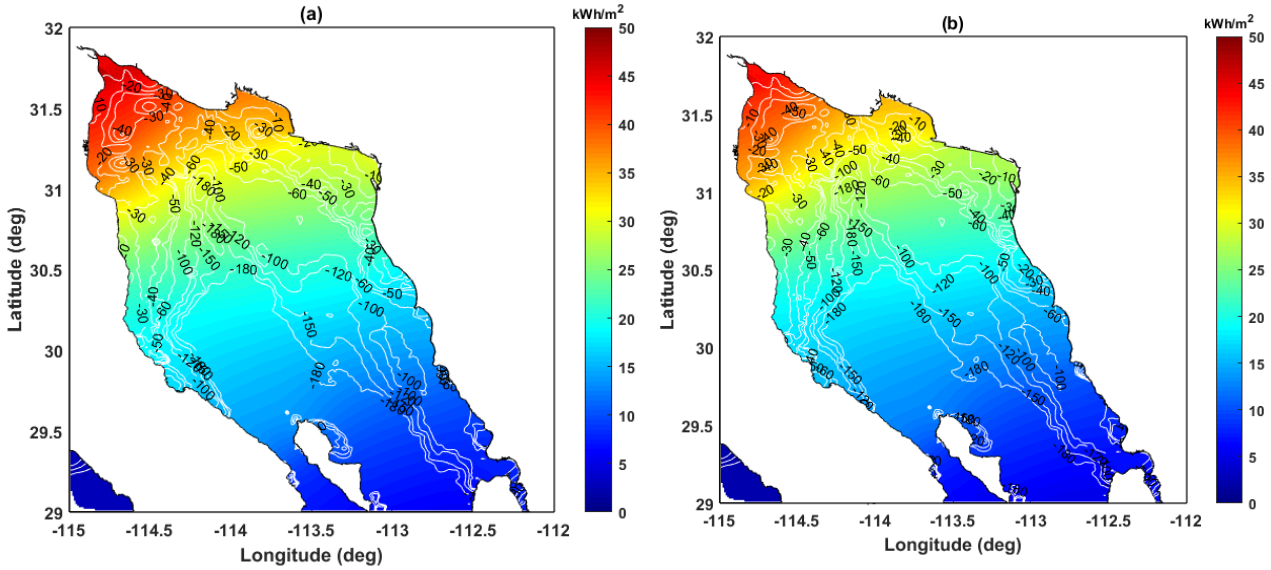

Fig. 9: Annual energy yield (a) all model constituents (b) Using M_2 plus S_2. All plots use the GEBCO data merged with the higher resolution data from CICESE, for the northern Gulf of California, with the bathymetry contours are overlaid as white lines.

Three different bathymetry products were used to estimate the theoretical annual energy yield and the contrasting results are shown in Fig. 10. It is clear the resource estimates are underestimated when the freely available global bathymetry products (e.g., GEBCO and ETOPO) are used on their own. The ETOPO bathymetry gives a maximum resource of 28 kWh/m^2 (Fig. 10b) in the northern region, while the GEBCO bathymetry gives a maximum

resource of 20 kWh/m^2 in this area (Fig. 10c). These are almost 50% of that estimated when we combine the higher resolution CICESE bathymetry data with GEBCO (Fig.10a).

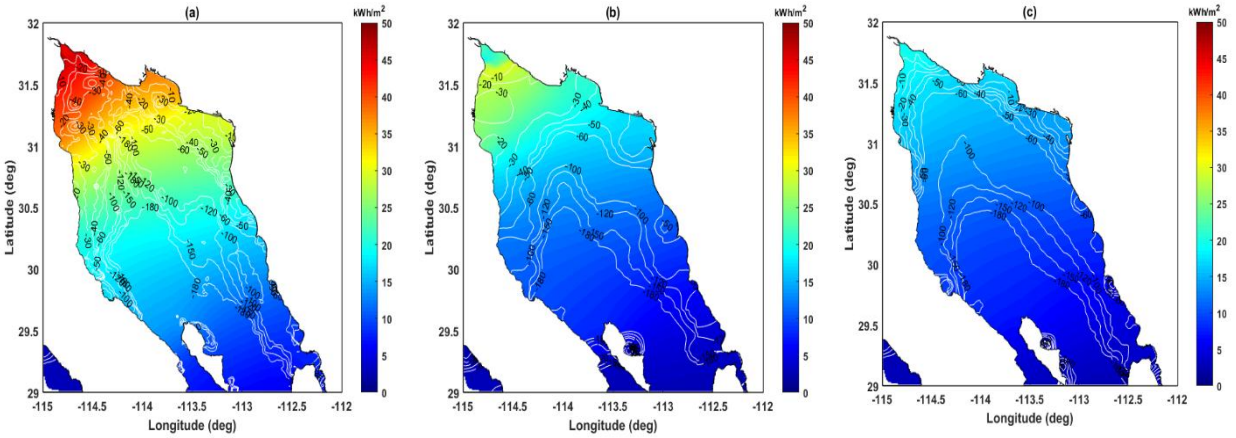

Fig. 10: Annual energy yield using different bathymetry products: (a) GEBCO+CICESE (b) ETOPO and (c) only GEBCO with the Bathymetry contours are overlaid as white lines.

4.3 Tidal power technical output

The third objective was to determine the energy that can be technically exploited whilst considering different operational strategies and certain tidal range power plant technical specifications. In Fig. 8a to 8d we consider the tidal signal and the theoretical energy accumulated in each cycle in sites of interest in the GC. Fig. 8e appends results to be used as a reference based on the theoretical energy from a site where a tidal lagoon proposal has been extensively studied, the Swansea Bay area in the Bristol Channel of the UK [47][48]. By observation, the GC is far less energetic in all four locations and this can also be appreciated in Table 4. The tidal range is 30-38% less than for the reference site in the UK. However, this difference corresponds to a 47-59% reduction in the theoretical energy, attributed to the non-linear relationship between the tidal range and the available theoretical energy (see Eq. 1).

Operational modelling sheds further insights into how tidal power plants would perform in the GC. The power output from each of the three strategies is summarised in Fig. 11 where the intervals for power generation can be calculated more accurately. As with every tidal energy technology, far less energy is available during neap tidal conditions, with shorter intervals of power generation. One-way operation generates energy only on the incoming (flood) or outgoing flow (ebb) tide while two-way operation produce energy during both

periods (ebb and flood) [6]). Two-way generation delivers four pulses of energy over 24h which helps distribute the tidal power contributions. Two-way generation with pumping corresponds to a superior performance but this comes with the requirement that energy is invested to pump water and increase the head difference that turbines will then generate [9] from as illustrated in Fig. 11.

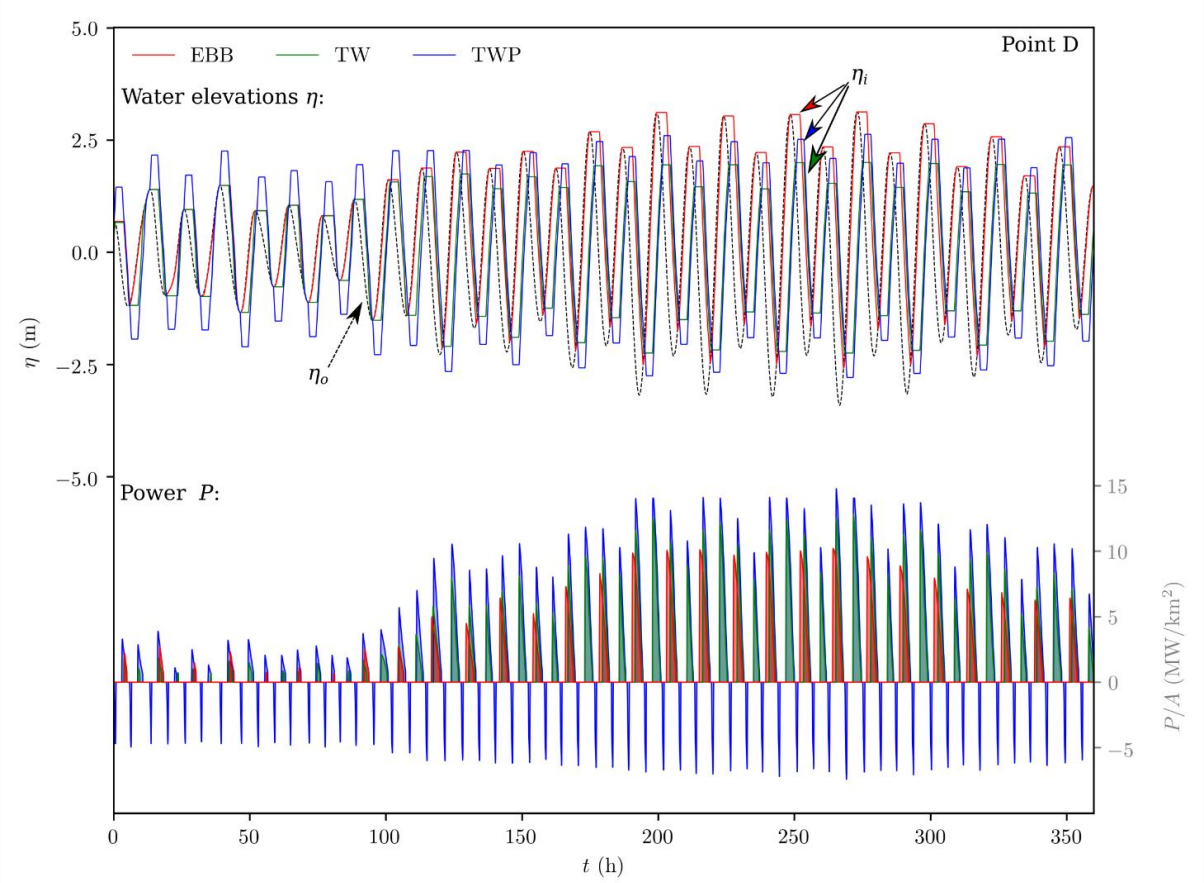

Fig. 11: Water elevations and power produced for the three operational strategies for point D (Gulf of Santa Clara). EBB= Ebb-only generation, TW= Two-way generation, TWP = Two-way generation with pumping. η_ι = inner water elevations, η_o = outer water elevations. Negative values in the power scale comes from pumping.

Even though it can be observed that energy can indeed be harnessed from the tides in the Gulf of California, there are significant efficiency losses as summarised in Table 4. The power plants consistently perform worse based on the maximum available head at any given site (in this work, the GC in Mexico site relative to the reference one in Swansea Bay). The performance aspect is highly associated with the head differences between the turbine deployment and the head available at site. By observing the hill chart in Fig. 5, the efficiency of practical turbine designs increases with an ascending head difference. The lower efficiency

can be observed by the significantly greater discharge of Q_{chart} relative to $Q_{ideal.,}$ where in the latter hydraulic and other losses are not taken into account. More details on the bulb turbine performance efficiency for tidal range structures can be found in [46]. The best performing site in the GC is the Gulf of Santa Clara (Point D in Fig. 8 & 11) which delivers 50%, 40% and 33% of the energy relative to the reference site for ebb-only, two-way and two-way with pumping strategies respectively.

5. Discussion

In this paper, we have undertaken a detailed quantification of the theoretical and technical tidal range energy resource available in the northern part of the GC. Although a number of parameters are significant in tidal range energy resource assessments, the most important is clearly tidal range. In this study, we mapped tidal range throughout the GC using results from a validated hydrodynamic numerical model. The maximum tidal range is up to 8 m in the northern most part of the GC, in the vicinity of the Gulf of Santa Clara and San Felipe Bay. However, the mean annual tidal range is closer to 5 m in this region.

The annual energy (density) yield ranges from 20 to 50 kWh/m^2 in the northern part of the GC. The maximum values are between 45 and 50 kWh/m^2 in the vicinity of the Gulf of Santa Clara, where the tidal range is the largest. For comparison, the annual energy yield estimated for areas with the world's largest tidal ranges by [14] (e.g. Hudson Bay, Canada; Bristol Channel, UK; Patagonian Shelf; North-western Australian Shelf) is of order 100 kWh/m^2 or larger. Also in the study conducted by [14] suggest a minimum acceptable annual yield of 50 kWh/m^2, with a maximum water depth of 30 m (based on construction costs of the embankment being prohibited in deeper waters. In the vicinity of the Gulf of Santa Clara and San Felipe Bay these criteria are just met.

We determined the energy that can be technically converted at four sites (locations shown in Fig. 1b). We considered different operational strategies (e.g. flood versus ebb generation) and certain tidal range power plant technical specifications. We contrasted these sites with the proposed tidal lagoon in Swansea Bay in the Bristol Channel of the UK, which has been extensively studied (e.g. [47] [48]). The best performing of the four selected sites in the GC is Gulf of Santa Clara (Point D in Fig. 8 & 11). This site has the best performing delivering technically annual energy output of 125 GWh (ebb-only), 159 GWh (two-way) and 174 GWh (two-way with pumping operational scheme) which represent 50%, 40% and 33%

respectively of the absolute power relative to a much studied reference site (Swansea Bay in the UK) utilizing similar impounded area. In this study we have, for an early-stage assessment, used a 0-D modelling approach. This omits the influence of the structure on the localised hydrodynamics and assumes a constant impounded surface area with negligible water elevation variations in its interior [6]. The operational algorithms employed in 0-D (Fig. 4) have previously been linked with 2-D hydrodynamic models to quantify hydrodynamic implications associated with the construction of tidal range structures [48], [27] and [49]. Comparisons between the two approaches (0-D and 2-D) suggest that similar findings can be obtained when assessing small-scale projects under certain conditions, and are certainly less than uncertainty due to storm surges [42]. A positive agreement has been observed for schemes that do not feature extensive intertidal regions upstream [14]. In contrast, caution has been advised for larger schemes such as with the Severn Barrage STPG proposal in the UK (impounding approximately 573 km^2, [50]), or for multiple medium-sized schemes operating concurrently. Discrepancies have been reported in the case of designs that occupy significant proportions of estuarine regions that are tidally affected and with a substantial proportion of the impounded area comprising shallow water regions susceptible to extended periods of exposure. Larger impoundments are expected to correspond to a noticeable impact on the estuarine tidal resonance by compromising the established evolution and reflection of the tidal waves, thus markedly altering the downstream tidal conditions that drive the operation and dictate the extractable energy resource. In contrast, schemes that comprise extensive shallow water regions might experience non-linear and rapid surface area changes that would simply not be included through a 0-D methodology.

As we previously highlighted in relation to tidal-stream energy within the GC study conducted by [19], grid connectivity in the region presents an additional challenge. The nearest electricity connection point to the Mexican national network is located in Sonora County, which is ~450 km from Playa Encanto. North of the GC there are two electricity connection points on the Mexican/US border, but these are not connected to the national Mexican network. These points are located ~200 and ~370 km to San Felipe Bay. Difficult access to this region, due to its topography, lack of fresh water and dry weather make this area unattractive for urban development. Furthermore, all the four selected sited would be closely in phase with one another (Fig. 8a-d). Therefore, the tidal-range energy that could be could be converted into electricity from the GC might be more suitable for off-grid applications.